Joule

CellPress

Article

Toward abiotic sugar synthesis from CO_2 electrolysis

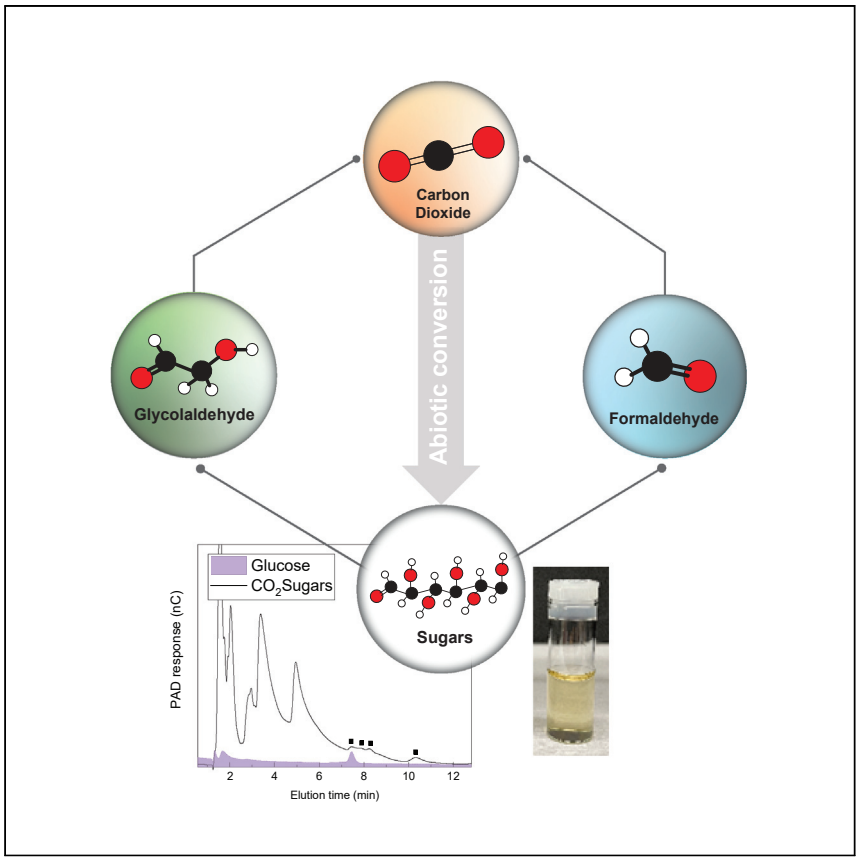

CO_2 upcycling has traditionally stopped at simple hydrocarbons and oxygenates, leaving CO_2 conversion to complex products like sugars to biological organisms. The timescales, stabilities, and efficiencies associated with biological CO_2 upconversion may not be sufficient to scale up waste CO_2 utilization and mitigate CO_2-derived climate change. We show and experimentally evaluate an abiotic path toward sugar generation from CO_2, linking existing electroconversion platforms and prebiotic chemistry.

Stefano Cestellos-Blanco, Sheena Louisia, Michael B. Ross, ..., Jessica N. Cestellos Spradlin, Daniel K. Nomura, Peidong Yang

p_yang@berkeley.edu

Highlights

A roadmap of CO_2 upcycling modules leading to abiotic sugar generation was established

CO_2 electroconversion to formaldehyde and glycolaldehyde was experimentally assessed

Glycolaldehyde from CO_2 initiated sugar formation in a chemically complex medium

Sugars initiated by CO_2-derived glycolaldehyde served as feedstock for *Escherichia coli*

Cestellos-Blanco et al., Joule 6, 2304–2323
October 19, 2022
https://doi.org/10.1016/j.joule.2022.08.007

CellPress

Joule

Article

Toward abiotic sugar synthesis from CO_2 electrolysis

Stefano Cestellos-Blanco,[1,2,7] Sheena Louisia,[3,4,7] Michael B. Ross,[3,8] Yifan Li,[3,4] Nathan E. Soland,[3] Tyler C. Detomasi,[3] Jessica N. Cestellos Spradlin,[3] Daniel K. Nomura,[3,5] and Peidong Yang[1,2,3,4,6,9,*]

SUMMARY

Although steady progress has been achieved toward upcycling waste CO_2 through diverse catalytic strategies, each approach has distinct limitations, hampering the generation of complex products like sugars. Here, we provide a roadmap that evaluates the feasibility associated with state-of-the-art electrochemical processes eligible for converting CO_2 into glycolaldehydes and formaldehydes, both essential components for sugar generation through the formose reaction. We establish that even in low concentrations, glycolaldehyde plays a crucial role as an autocatalytic initiator during sugar formation and identify formaldehyde production as a bottleneck. Our study demonstrates the chemical resilience of the formose reaction successfully carried out in the chemically complex CO_2 electrolysis product stream. This work reveals that CO_2-initiated sugars constitute an adequate feedstock for fast-growing and genetically modifiable *Escherichia coli*. Altogether, we introduce a roadmap, supported by experimental evidence, that pushes the boundaries of product complexity achievable from CO_2 electroconversion while integrating CO_2 into life-sustaining sugars.

INTRODUCTION

As an abundant and inexpensive waste product, CO_2 is an attractive feedstock to produce functional chemicals and materials.[1–3] For example, CO_2 is a prime target for *in situ* resource utilization (ISRU) on Mars to enable crewed deep space exploration.[4–7] A self-sustaining infrastructure dedicated to producing mission-critical elements would reduce mission costs over the long term, increase operational resilience, and protect crew well-being thus allowing for unprecedented planet exploration.[6] In addition, sequestering waste CO_2 through its utilization could prevent further terrestrial atmospheric accumulation of this greenhouse gas.[8] Electrochemical CO_2 reduction reaction (CO_2RR) platforms can be powered modularly by any electricity source and thus be sustained by renewable solar or wind energy sources, offering a promising way to close the loop of the carbon cycle.[9] Although electrocatalytic optimization has been successful for the generation of the main 2 e^- reduction products, carbon monoxide (CO) and formate ($HCOO^-$), the formation of higher-order products has remained a challenge.[10–12] Cu is the only element that displays a high turnover rate toward multi-carbon (C_{2+}) products at reasonable overpotentials.[13,14] However, limited progress has been made to boost its selectivity toward C_{2+} molecules due to the complexity of favoring one of the many possible reaction pathways. Additionally, CO_2 has rarely been converted into molecules larger than three carbons due to the difficulty for one surface to successively facilitate multiple steps which individually require distinct energy requirements.[15–19]

CONTEXT & SCALE

The conversion of CO_2 to drop-in and complex products would be transformative to the field of CO_2 upcycling. However, limited progress has been achieved using heterogeneous catalysts due to the complexity of favoring one out of the many possible reaction pathways and associated high energy penalties. Here, we establish a pathway toward the generation of a complex product in sugars from CO_2 by sequentially combining existing CO_2 conversion modules. Initial CO_2 products in glycolaldehyde and formaldehyde react together through the formose reaction to generate sugars. We experimentally evaluated commonly reported electrochemical platforms for formaldehyde and glycolaldehyde production from CO_2. As a result, we determined that glycolaldehyde even in low quantities is a necessary initiator for sugar formation. Sugars could be an important feedstock in biomanufacturing; therefore, we demonstrated that sugars formed with CO_2-derived glycolaldehyde could be used as feedstock.

CO_2 bio-electrosynthesis employing autotrophic bacteria as biocatalysts is a complementary approach to the purely inorganic catalyst-mediated electrochemical CO_2RR affording high selectivity to C_{2+} products.[20,21] However, CO_2 turnover rates for autotrophic bacteria are orders of magnitude lower than those from heterogeneous electrochemical CO_2 reduction due to their sluggish autotrophic metabolism, and the requirement to maintain biocompatible conditions within the electrochemical set-up.[22,23]

The ability to leverage the independent strengths of inorganically catalyzed CO_2 reduction and biocatalysis would be transformative, enabling scalable CO_2 reduction with selective production of complex, multi-carbon products. For this reason, platforms combining inorganic CO_2RR and whole-cell biocatalysis have been reported.[24–27] More precisely, biocatalysts upgrade CO_2-derived CO, $HCOO^-$, or acetate to higher-value products such as alcohols and bioplastics. However, these lower energy and growth-inhibiting feedstocks may limit the scalability of this process.[28,29] Biological organisms commonly rely on carbohydrates as an energy-dense carbon source.[30] In fact, sugars are a primary feedstock in the bioindustry, and humans rely on carbohydrates as a constitutional dietary staple.[31,32] Recently, researchers have reported non-photosynthetic carbohydrate generation from CO_2 through engineered *in vitro* enzymatic pathways or mediated by genetically engineered, whole-cell microorganisms.[27,33] However, abiotic sugar synthesis from CO_2 remains unreported. Leveraging high-rate inorganically catalyzed CO_2RR to create sugar feedstocks could be a disruptive technology. To encourage scientists to pursue this objective, the National Aeronautics and Space Administration (NASA) launched a Centennial Challenge focused on abiotically converting CO_2 to carbohydrate sugars.[34] These could be employed as a high-energy feedstock for fast-growing and genetically modifiable bacteria like *Escherichia coli* (*E. coli*) enabling chemical and material biomanufacturing during deep space crewed missions.

Here, we provide a roadmap for coupling diverse chemical modalities to enable abiotic CO_2-to-sugar conversion. From this overview, we identified a direct all-electrochemical route to supply aldehyde precursors in formaldehyde and glycolaldehyde from CO_2 that, when combined with a divalent metal catalyst through the formose reaction, react to form high-order sugars including glucose. Next, we experimentally evaluated the electrochemical platforms required to supply formaldehyde and glycolaldehyde from CO_2. We used a Cu nanoparticle (NP) ensemble electrocatalyst well-suited for the CO_2 electroconversion to glycolaldehyde.[35,36] Other than Cu-based CO_2RR, there is no clear one-pot CO_2 to glycolaldehyde conversion process.[37,38] Although we demonstrated formaldehyde electroproduction from CO_2 on a boron-doped diamond (BDD) electrode,[39] its productivity was too low to feasibly sustain the formaldehyde requirement of the formose reaction. Herein, we point to avenues for potential improvement in electrochemical formaldehyde production to promote higher interest in this valuable product by the CO_2 electrochemistry community. Unlike glycolaldehyde, there are various well-established electro- and thermochemical approaches to generate formaldehyde from CO_2 (Figure 1; Table 1). For this reason, we employed commercially available formaldehyde as a stand-in and focused on studying the feasibility of coupling heterogeneous electrocatalysis with the formose reaction. Our study demonstrates for the first time the chemical resilience of the formose reaction which was achieved in a chemically complex environment. We establish the feasibility of employing glycolaldehyde, a minority molecule derived from CO_2 electroreduction, that is necessary initiator of the autocatalytic pathway of the formose reaction. Specifically, without CO_2-derived glycolaldehyde as an autocatalytic initiator, the formose reaction did not yield

[1]Department of Materials Science and Engineering, University of California, Berkeley, Berkeley, CA 94720, USA

[2]Center for the Utilization of Biological Engineering in Space (CUBES), University of California, Berkeley, Berkeley, CA 94720, USA

[3]Department of Chemistry, University of California, Berkeley, Berkeley, CA 94720, USA

[4]Chemical Sciences Division, Lawrence Berkeley National Laboratory, Berkeley, CA 94720, USA

[5]Department of Nutritional Science and Toxicology, University of California, Berkeley, Berkeley, CA 94720, USA

[6]Kavli Energy Nanosciences Institute, Berkeley, CA 94720, USA

[7]These authors contributed equally

[8]Present address: Department of Chemistry, University of Massachusetts, Lowell, Lowell, MA 01854, USA

[9]Lead contact

*Correspondence: p_yang@berkeley.edu

https://doi.org/10.1016/j.joule.2022.08.007

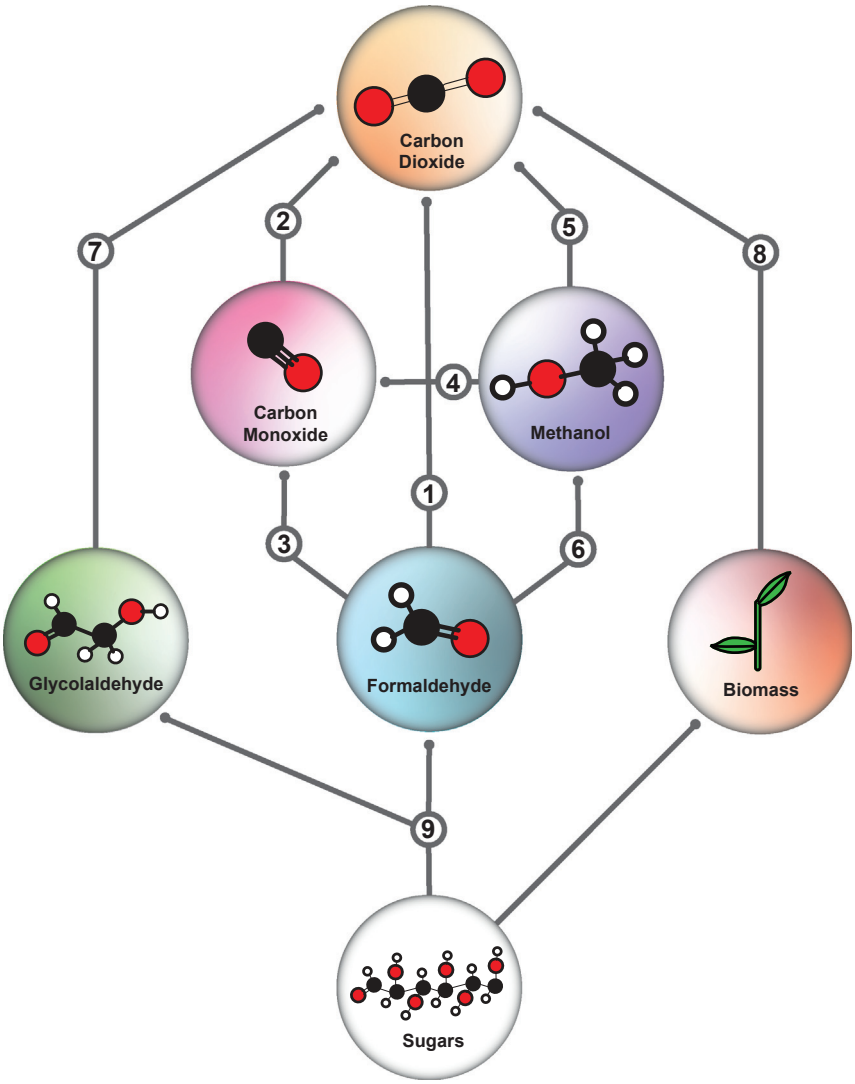

Figure 1. CO_2-to-sugar conversion roadmap

Overview of eligible chemical pathways to produce precursor aldehydes in formaldehyde and glycolaldehyde to form sugars through the formose reaction (9). Each pathway indicates a conversion platform, with electrochemical and thermochemical production metrics for pathways 1–7 presented in Table 1. Pathways 8 and 9 represent CO_2-to-biomass conversion through natural photosynthesis and aldehyde-to-sugar conversion through the formose reaction, respectively.

sugars. Finally, we devised a simple method to prepare the CO_2-initiated formose sugars for use as feedstock in an *E. coli* culture. The *E. coli* culture proliferated when fed with formose sugars, representing one of the first demonstrations of using abiotically formed sugars to successfully sustain life. Altogether, we showcase a synthetic route to incorporate CO_2 electrolysis products into the production of life-sustaining sugars while pointing out the understudied areas necessary to address before fulfilling a complete abiotic CO_2-to-sugar conversion.

RESULTS AND DISCUSSION

Roadmap to abiotic sugar synthesis

Abiotic sugar synthesis from CO_2 could provide an avenue for drop-in chemical, material, fuel, and even food production.[7,52,53] Currently, agriculture provides all

Table 1. Detailed summary of the paths toward sugar precursors as illustrated in Figure 1

Conversion	Process	Catalyst	Conditions	Efficiency/ selectivity	Production rate	Reference
(1) CO_2 → formaldehyde	thermochemical[a]	$PtCu/SiO_2$	150°C, 6 atm	N/A	~52.2×10^{-4} mol g_{cat}^{-1} h^{-1}	Lee et al.[40]
(1) CO_2 → formaldehyde	electrochemical[a]	boron-doped diamond	− 1.5 V versus Ag/AgCl	FE: ~62%	3.75×10^{-4} mol h^{-1}	Nakata et al.[39]
(2) CO_2 → CO	thermochemical[b]	$Pd/CeO_2/Al_2O_3$	250°C, 1 bar	PS: 87%	1.62×10^{-4} mol g_{cat}^{-1} h^{-1}	Daza and Kuhn[41]
(2) CO_2 → CO	thermochemical[b]	$La_{0.75}Sr_{0.25}FeO_3$	550°C, 1 bar	PS: 95%	0.13 mol g_{cat}^{-1} h^{-1}	Daza and Kuhn[41]
(2) CO_2 → CO	electrochemical[b]	Ag NPs	E_{cell} = 2.5 V (GDE)	FE: 99% EE: 53%	7.8×10^{-3} mol cm^{-2} h^{-1}	Bhargava et al.[42]
(3) CO → formaldehyde	thermochemical[a]	$Ru-Ni/Al_2O_3$	80°C, 100 bar, aqueous	PS: ~100%	63.2×10^{-6} mol L^{-1} g_{cat}^{-1} h^{-1}	Bahmanpour et al.[43]
(3) CO → formaldehyde	electrochemical[a]	MoP	~20°C, H UPD (−30 mV versus RHE)	FE: ~96%	1.8×10^{-4} mol g_{cat}^{-1} h^{-1}	Yao et al.[44]
(4) CO → CH_3OH	thermochemical[b]	$Cu/ZnO/Al_2O_3$	~240°C, with H_2 co-feed	N/A	2.5 kg L^{-1} h^{-1}	Herman et al.[45]
(4) CO → CH_3OH	electrochemical[a]	CoPc	−0.64 V versus RHE	FE: ~14%	6.3×10^{-6} mol cm^{-2} h^{-1}	Boutin et al.[46]
(5) CO_2 → CH_3OH	thermochemical[b]	Cu/ZnO/AlOOH	250°C, 50 atm with H_2 co-feed	56 C-mol % selectivity, 14.1% yield	10.9 mmol g_{cat}^{-1} h^{-1}	Choi et al.[47]
(5) CO_2 → CH_3OH	electrochemical[a]	$Cu_{2-x}Se$ NPs	−2.1 V versus Ag/Ag^+ ACN/H_2O	FE: ~78%	2×10^{-4} mol cm^{-2} h^{-1}	Yang et al.[48]
(6) CH_3OH→ formaldehyde	thermochemical[b]	Ag crystals (ballast)	600°C –700°C, 1 atm	PS: 87%	N/A	Sperber[49]
(6) CH_3OH → formaldehyde	thermochemical[b]	$Fe_2(MoO_4)_3$ (Formox)	250°C –400°C, 1 atm	PS: ~99%	N/A	Bahmanpour et al.[50]
(6) CH_3OH → formaldehyde	electrochemical[a]	Pt (polycrystalline, disc)	0.25 V versus Ag/AgCl (0.1 M $HClO_4$)	FE: ~38%	1.8×10^{-8} mol cm^{-2} h^{-1}	Korzeniewski and Childers[51]
(7) CO_2 → glycolaldehyde	electrochemical[b]	Cu NPs	−0.81 V versus RHE (0.1 M $KHCO_3$)	FE: ~0.2%	N/A	Kim et al.[35]

The number in parenthesis is associated with the conversion step in Figure 1. For each module, reported operating conditions are shown along with productions rate and product selectivity. NPs, nanoparticles; FE, faradaic efficiency; PS, process selectivity; EE, energy efficiency; RHE, reversible hydrogen electrode; H UPD, hydrogen underpotential deposition; GDE, gas diffusion electrode; ACN, acetonitrile.

[a]Denotes a nascent conversion process with few or singular supporting reports.

[b]Indicates a well-established or industrially validated catalytic process.

commercial sugar feedstocks. However, this sector is heavily reliant on government subsidies, is often the source of unfair labor practices, occupies large arable swaths of land, consumes large amounts of water, requires pesticide and fertilizer use, and finally as a monoculture is vulnerable to pests and disease.[54–58] Therefore, it would be beneficial to develop an independent sugar generation platform that requires only H_2O, CO_2, and renewable electricity.

A complete abiotic CO_2-to-sugar conversion platform has yet to be developed. Furthermore, a one-pot, direct CO_2-to-sugar conversion is unlikely to be feasible due to the manifold reaction steps required to transform CO_2 to molecules with ordered C–H, C–O, and C–C bonds. However, keeping the reaction cascade concise would improve its scalability. Therefore, we reverse engineered a reaction pathway to sugars. Sugars, although complex, consist of C, H, and O backbones. We were inspired by prebiotic chemistry to consider approaches through which simple C_1 and C_2 oxygenates could be put together into sugars.[59] We singled out the formose reaction as a promising avenue for sugar generation from simple molecules. In the formose reaction, aldehydes are combined in the presence of a divalent metal cation to produce sugars.[60] Historically, formaldehyde has provided the main carbon precursor for the formose reaction. However, more recent studies have determined that an organic initiator such as glycolaldehyde capable of enediolization is required to achieve an appreciable rate of sugar generation.[61–63] Therefore, we identified our initial targets in formaldehyde and glycolaldehyde.

To engineer our CO_2-to-sugar pathway, we carefully considered widely reported avenues for the abiotic conversion of CO_2 to formaldehyde and glycolaldehyde (Figure 1). As previously stated, the only clear one-pot CO_2-to-glycolaldehyde heterogeneous conversion catalysts are Cu electrocatalysts. There are no reports for the efficient, heterogenous, and thermocatalytic conversion of CO_2 to glycolaldehyde. Although the electrochemical conversion efficiency to glycolaldehyde is low, only a minimal amount of glycolaldehyde is required to autocatalyze the formose reaction. On the other hand, there are several avenues to convert CO_2 to formaldehyde.

These avenues may be thermochemical, electrochemical, or a combination thereof, depending on practical concerns of the total process. It is desirable to select a synthesis route that is sufficiently simple, efficient, robust, and productive. We thus attempt to illustrate several of these options in Figure 1. Among them is the work of Nakata and coworkers that demonstrates the only single-step heterogeneous CO_2-to-formaldehyde electroreduction.[39] This involves a BDD electrode for which the faradaic efficiency (FE) is ~62% in aqueous conditions. The rates of production achieved in this work (i.e., order of $\mu A.cm^{-2}$) are however not practical for scale up. Additionally, the single-step 4 e^- reduction imposes significant thermodynamic challenges, and often, its productivity is limited by the low stability of formaldehyde especially in aqueous media. It is worth noting that although $HCOO^-$ has been suggested to be an intermediate in this work, there are no other notable reports supporting the electrochemical reduction of $HCOO^-$ to formaldehyde as a viable process. This remark is also applicable to a thermocatalytic approach involving the conversion of $HCOO^-$ to formaldehyde. Moreover, despite a few isolated reports, the thermocatalytic conversion of CO_2 to formaldehyde has not been well established. Therefore, we explored alternative, albeit staged, pathways to formaldehyde (Table 1).

CO_2-derived products including methanol (CH_3OH) or CO can for instance be converted to formaldehyde. Electrocatalytically, the 2 e^- reduction from CO_2 to CO

presents a clear advantage as a more thoroughly studied reaction. Consequently, this reaction has been optimized with high production rates and reasonable energy efficiencies when carried out in a gas diffusion cell configuration.[16,64] Furthermore, a molybdenum phosphide catalyst has recently been reported to readily convert CO to formaldehyde in aqueous electrolyte at low overpotentials under ambient conditions.[44] Although understudied, this electrocatalytic pathway offers a selective yet energetically less demanding alternative than a thermocatalytic counterpart operating at 90°C and 100 bar. Further investigations should thus consider the tandem electrocatalytic conversion of CO_2 to CO to formaldehyde as a viable formaldehyde electrosynthetic route.

We considered another route that involves the sequential production of CH_3OH before further oxidation to formaldehyde. However, in contrast to the CO_2 electroreduction to CO, the selective 6 e^- electroreduction of CO_2 to CH_3OH is inherently more challenging. Although some reports highlighted FEs as high as 97%, the stable and efficient formation of CH_3OH remains elusive.[65,66] The electrooxidation of CH_3OH also remains greatly limited with FE as low as 38% at 0.25 V versus Ag/AgCl.[51] Alternatively, the two-step thermochemical approach may be more realistic where both the CO_2 conversion to CH_3OH and subsequent partial oxidation to formaldehyde have been carried out with relatively high process efficiencies. The partial oxidation of CH_3OH to formaldehyde is for example carried out industrially at a 60 million metric tons per year scale through the ballast or Formox processes catalyzed by silver or iron molybdate, respectively.[67–69]

The different routes from CO_2 leading to formaldehyde can be quantitatively compared using Table 1 which summarizes representative electrochemical and thermochemical catalysts and their efficiencies and productivities. First, given the advantages of electrochemistry over thermochemistry including mild reaction conditions, low capital costs, and easy integration into the power grid,[70] we chose to evaluate an electrocatalytic route to obtain the formaldehyde building block. Second, although smaller sequential steps can be beneficial for their individual optimization, intermediary product separation and transfers introduce the risk of chemical incompatibility. Thus, with the desire to minimize reaction steps, we investigated the BDD platform for formaldehyde electroproduction. Finally, to highlight the energy efficiencies that need to be achieved by a solar-powered abiotic sugar synthesis to surpass the typical sunlight to biomass conversion efficiency of plants, we calculated an efficiency grid (Figure S1 and see supplemental experimental procedures). We determined that given a formaldehyde basis and despite a relatively large cell overpotential of 1.5 V, the abiotic approach could eventually surpass the crop solar energy conversion efficiency upon mastering and thoroughly standardizing CO_2 electroconversion to formaldehyde with FEs above 60%, as has been previously reported.[39]

CO_2 electrochemical reduction to aldehyde precursors

The electrochemical reduction of CO_2 on Cu catalysts yields more than 16 different products with aldehydes often contributing to less than 5% of the total FE.[18] The formation of surface bound CO (*CO) intermediates and subsequent C–C coupling are both necessary steps for the mechanistic pathway leading to the formation of aldehydes and further reduced C_{2+} products (Figure 2A). However, after C–C coupling, aldehydes are expected to be further reduced which is likely the reason for their overall lower efficiency.[71–73] Consequently, catalysts that have been reported with high FE for C_{2+} products, and especially for C_{2+} oxygenates, are more likely to produce an intermediate species like glycolaldehyde. The Cu NP ensemble previously reported in our group (Figure 2B) is therefore an ideal candidate to optimize the

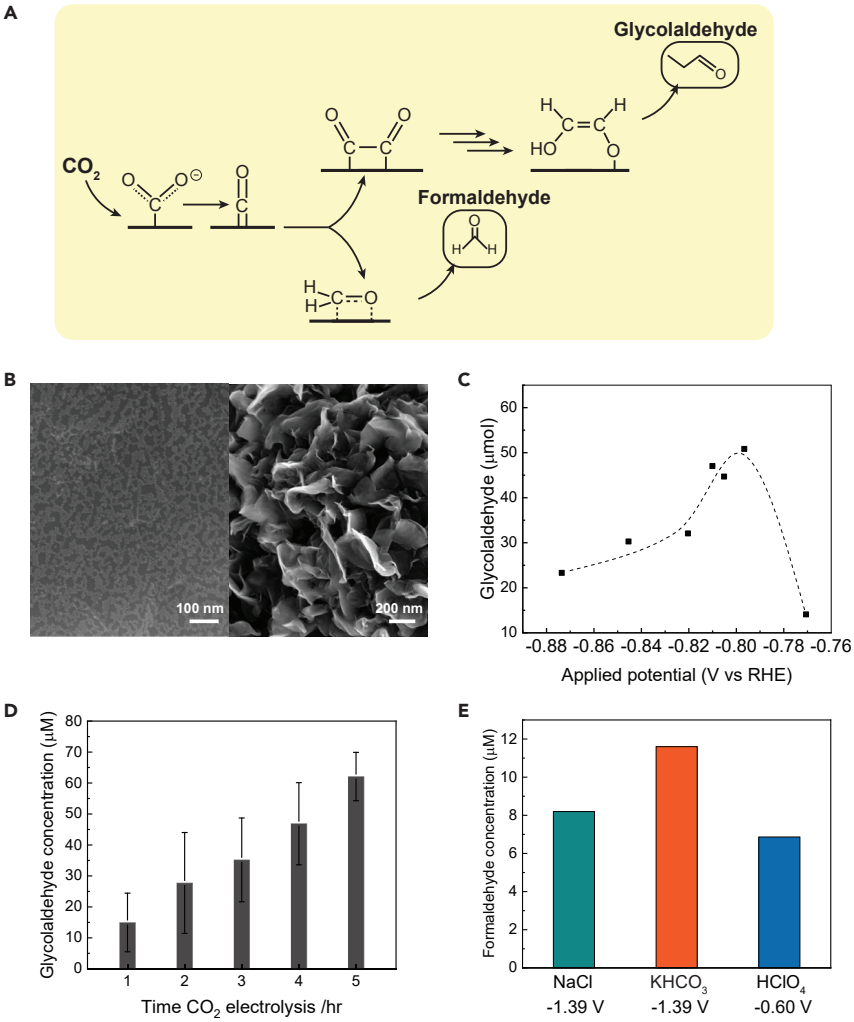

Figure 2. CO_2 electrolysis produces upgradable aldehydes

(A) Scheme of the mechanistic pathway of CO_2 electroreduction to glycolaldehyde and formaldehyde.

(B) SEM of the Cu NP ensemble (left) and the BDD (right) electrocatalysts.

(C) Concentration of glycolaldehyde obtained after 4 h of CO_2 electrolysis in 0.1 M $KHCO_3$ using the Cu NP ensemble at various applied potentials.

(D) Accumulation of glycolaldehyde produced at −0.80 V versus RHE as a function of electrolysis time using the Cu NP ensemble in 0.1 M $KHCO_3$.

(E) Concentration of formaldehyde obtained after 1 h of CO_2 electrolysis using a BDD electrode in 0.1 M NaCl, $KHCO_3$, and $HClO_4$ electrolytes. All applied potentials are reported on the RHE scale. Error bars are one standard deviation of three independent measurements.

production of glycolaldehyde due to its high intrinsic activity for CO_2-to-C_{2+} conversion at low overpotential (i.e., partial current density per surface Cu atom 7-fold greater than traditional Cu foil at −0.80 V versus reversible hydrogen electrode [RHE]).[35,36] The catalytic properties of this Cu NP ensemble toward glycolaldehyde specifically sits in a favorable range both in terms of selectivity (FE) and activity (current density) when compared with other Cu-based catalysts (Figures S2 and S3). We evaluated the performance of the Cu NP ensemble across different applied potentials to maximize the rate of CO_2-to-glycolaldehyde production. We identified the peak production to reach 12 $\mu g.h^{-1}$ at −0.80 V versus RHE (Figure 2C) which for a

68.9 μg loading of Cu corresponds to 0.17 $g.h^{-1}.g_{Cu}{}^{-1}$. An increase or decrease in the overpotential is likely more favorable to the reduction of produced aldehydes or the hydrogen evolution reaction (HER), respectively. Indeed, the peak production of glycolaldehyde occurs at a more positive potential than ethylene and ethanol further suggesting that a too negative applied potential will further reduce any produced aldehydes (Figure S4).

Given the optimal applied potential, we then investigated how to further maximize the concentration of glycolaldehyde. The CO_2RR activity of the Cu NP ensemble remains steady after hours of operation as demonstrated by the stable current density and product distribution monitored by gas chromatography (GC) (Figures 2D and S5). Although the concentration of aldehyde increases linearly up to 5 h of electrolysis, we observe a decline after 8 h (Figure S6). The interrupted accumulation of aldehyde is likely due to their propensity toward further reduction to alcohol or alkene over time.[71–73] Despite our optimization of the CO_2 electroconversion to glycolaldehyde, the reaction is inherently limited, and the FE of this process has rarely been improved beyond 2%–3%. As a result, we considered 4 h CO_2RR adequate to consistently obtain a sufficiently high concentration of glycolaldehyde to initiate the autocatalysis of formaldehyde while minimizing the risk of further glycolaldehyde reduction due to elongated time of CO_2 electrolysis. Consequently, we explored the conversion path from CO_2 to the other sugar precursor in formaldehyde.

Traditionally, formaldehyde is derived from syngas or CH_3OH through well-established industrial synthetic processes.[67–69] Nakata et al. have presented a promising electrocatalytic avenue to convert CO_2 to formaldehyde with a FE of 62% using a BDD electrode in aqueous conditions (FE 74% in CH_3OH electrolyte).[39] Inspired by this demonstration, we combined previous insights obtained from CO_2 electroreduction on BDD to evaluate its potential for the aqueous production of formaldehyde (Figure 2B and see supplemental experimental procedures). We chose, in part, to evaluate the BDD platform experimentally as our analysis (Figure S1) demonstrates that the solar conversion efficiency of plant-derived sugar production could be nearly surpassed with the BDD, given the metrics reported by Nakata et al. However, using the same reaction conditions as reported by Nakata et al., we did not produce formaldehyde at a comparable FE (only 0.89% over 2 h), and the reaction was principally dominated by HER (Figures 2E and S7).[39] Given this low FE, the solar-driven abiotic production of sugar would not surpass natural photosynthesis, regardless of overpotential (Figure S1). Future work will require further investigation of the catalyst synthesis to enhance the selectivity. In addition, the high reactivity of formaldehyde exacerbated both under reducing conditions and in the presence of hydroxyl anions will require adjusted reactor and operation design to maximize the reaction turnover. Reducing conditions and the proximity to hydroxyl anions promote aldehyde disproportionation to primary alcohols and carboxylic acids.[74]

Although unable to generate formaldehyde in sufficient quantities to sustain sugar synthesis, we were able to identify a principal bottleneck and bring attention to the importance of developing the electroproduction of formaldehyde from CO_2. While promising in principle, BDD cathodes require more rigorous characterization, and their synthesis needs to be standardized before they can become widely adopted. More specifically, despite the prospects suggested by previous reports with FEs as high as 60% that could rival plant efficiency, achieving the CO_2 electroconversion to formaldehyde in high yields introduced several practical challenges. Given the limitation associated with the large-scale electroproduction of aldehydes from CO_2 identified in Table 1 and through our own experimental investigation, we

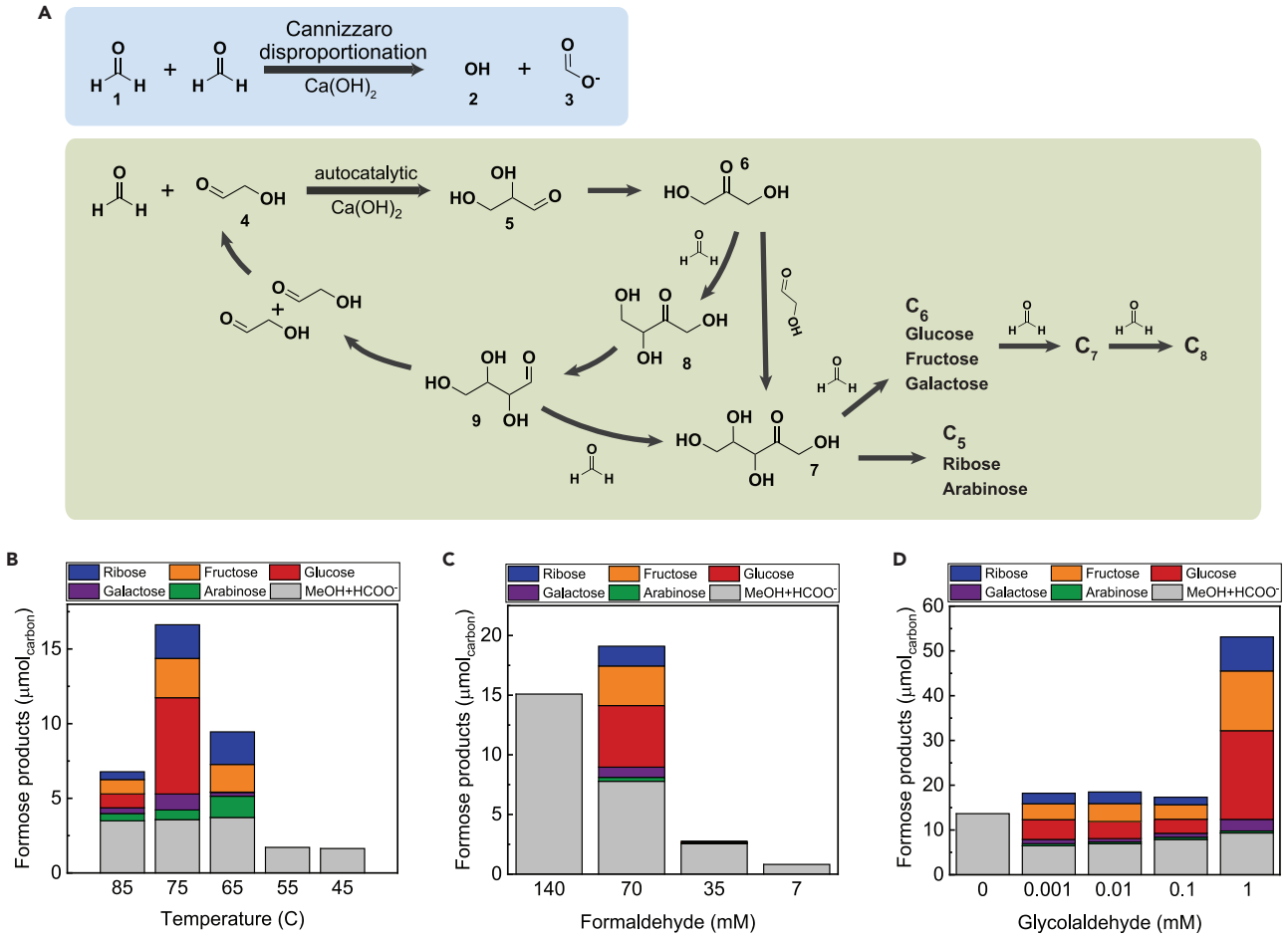

Figure 3. Formose reaction overview and optimization

(A) Upper inset: the Cannizzaro disproportionation of formaldehyde (1), methanol (2), and formate (3). In the absence of glycolaldehyde as an autocatalyst, the Cannizzaro reaction dominates in alkaline and aqueous conditions. Lower inset: overview of the formose reaction autocatalyzed with glycolaldehyde (4). Briefly, an aldol condensation of (1) and (4) generates glyceraldehyde (5), which undergoes an aldose-ketose isomerization to make dihydroxyacetone (6). (5) can be produced as either D- or L-glyceraldehyde. (6) and (4) react to form ribulose (7), which isomerizes to ribose among other C_5 monosaccharides. (6) may also undergo a further aldol condensation with (1) to make tetrulose (8), which isomerizes to aldotetrose (9). A retro-aldol reaction of (9) produces two molecules of (4), thus forming an autocatalytic cycle. (9) can also undergo an aldol condensation with (1) to produce (7). The resulting C_5 carbohydrates can sequentially undergo the same aldol condensation to produce C_6 carbohydrates which can themselves, through the same reaction, produce higher-order sugars (i.e., C_{7+}).

(B) Formose product distribution based on temperature with 100 μM glycolaldehyde and 70 mM formaldehyde.

(C) Formose product distribution with varying formaldehyde concentration with 100 μM glycolaldehyde at 75°C.

(D) Formose product distribution with varying glycolaldehyde concentration with 70 mM formaldehyde at 75°C. Sugars are quantified by HPAEC-PAD, and methanol and formate are determined by ^{1}H-NMR.

further examine the implications of low aldehyde concentrations during the formose reaction.

Sugar synthesis using the formose reaction

The formose reaction was established by Aleksandr Butlerov in 1861, although it received renewed attention in the 1950's and 60's principally led by Ronald Breslow and Alvin Weiss.[60,75–77] The reaction is catalyzed by a divalent metal cation (e.g., Ca^{2+}) under mild heating and alkaline conditions. Condensations and tautomerization of reactive intermediates convert aldehyde starting reactants into a mixture of sugars through a cyclical polymerization-like process (Figure 3A).[60] Although various

formose catalysts have been employed, we used Ca^{2+} as it is a low-cost and non-toxic catalyst, which is significant if the sugars are to be used as a feedstock in a bio-process.[77–79]

Having demonstrated CO_2RR for the generation of glycolaldehyde and formaldehyde, albeit in small quantities, we sought to verify the formose reaction conditions for the conversion of glycolaldehyde and formaldehyde to sugars. Before introducing the CO_2-derived aldehydes as reactants, and thus considering their low concentration limitation, we initially optimized the formose reaction with non-CO_2 derived standard samples of glycolaldehyde and formaldehyde. Although the formose reaction has been thought to start as the aldol condensation of two formaldehyde molecules to form glycolaldehyde, such direct dimerization only occurs in very specific conditions (i.e., in the gas-phase or under gamma-irradiation) and has been appraised in the literature as "chemically impossible" in the absence of glycolaldehyde in aqueous solutions.[61,80,81] Thus, the Cannizzaro disproportionation of formaldehyde dominates in an alkaline environment converting formaldehyde to CH_3OH and formic acid instead of sugars.[60,82] More recent reports categorically include an autocatalyst like glycolaldehyde or they start the formose reaction downstream of formaldehyde.[61–63] Consequently, we confirmed experimentally that formaldehyde alone with $Ca(OH)_2$ yields only CH_3OH and formic acid (Figures 3A and S8). The formose process can be initiated by adding glycolaldehyde, thus shortening the induction period and suppressing the competing Cannizzaro reaction.[80] Glycolaldehyde autocatalytically initiates the formose reaction cycle, in which formaldehyde condenses to a second molecule of glycolaldehyde. The autocatalytic cycle occurs at a much faster rate producing more glycolaldehyde which also reacts with other intermediates to form higher-order sugars. Sugars can arise from aldol condensations involving glycolaldehyde as the active methylene component and another aldehyde as the carbonyl component.[60] We found that in the absence of formaldehyde, glycolaldehyde alone can produce sugars confirming a sugar formation pathway through glycolaldehyde (Figures 3A and S8). Therefore, we verified that glycolaldehyde, even in trace quantities, is an essential autocatalyst for the formation of sugars thus confirming that electrochemical CO_2RR-derived glycolaldehyde (e-CO_2Glyc) is a necessary element for sugar production.

The formose reaction conditions were optimized to yield the highest quantity of biological feedstock products such as glucose (Figure 3). High-performance anion exchange chromatography with pulsed amperometric detection (HPAEC-PAD) was used for the separation and detection of a variety of carbohydrates of comparable weights (Figure 3 and see experimental procedures).[83] Unlike other analytical techniques, this separation allows for the identification of isomeric carbohydrates (i.e., glucose versus fructose) (Figure S9).

As a wide range of temperatures has been reported to enable the formose reaction, we tested a range from 45°C to 85°C in 10°C increments (Figure 3B).[84] A minimum temperature of 55°C was required to activate the reaction. Furthermore, 65°C yielded a higher proportion of C5 sugars (63%), whereas 75°C yielded more C6 sugars (78%). The total of 2.6 μmol sugars obtained at 75°C further decreases to 0.66 μmol at 85°C, as sugars may decompose into tar at the elevated temperature. We further determined the required concentration of formaldehyde to drive the formose reaction (Figure 3C). The Cannizzaro reaction dominates at concentrations below 35 mM as higher formaldehyde concentrations are needed to provide a driving force for C–C bond formation.[75] We found that a concentration of 70 mM formaldehyde adequately serves to synthesize feedstock sugar products. We

observed that formaldehyde concentrations starting at 140 mM do not adequately generate sugars. As has been previously described, this may be caused by an insufficient concentration of insoluble $Ca(OH)_2$ present to catalyze the reaction.[85] Finally, since the concentration of e-CO_2Glyc is low (~30 μM), it is essential to establish the minimum glycolaldehyde concentration necessary to autocatalyze the formose reaction. We determined this threshold concentration to be 1 μM as presented in Figure 3D. This is commensurate with glycolaldehyde provided by the CO_2RR. A higher total amount of sugars is obtained with higher glycolaldehyde concentrations (Figure 3D). In summary, in the adapted reaction conditions of 70 mM formaldehyde, 75°C and 10 μM glycolaldehyde among the biologically relevant sugars that we identified glucose is the major product (49%), followed by fructose (20%), ribose (17%), galactose (8%), and arabinose (5%).

CO_2 electrolysis product as a sugar-building block

After establishing the optimal conditions for the formose reaction, we tested whether CO_2RR-derived products could undergo the formose reaction. Our experimentally obtained formaldehyde concentration is too low to support the formose reaction as evidenced by Figure 3C. Alternative synthetic routes to obtain formaldehyde in high yields from CO_2 were discussed above (Figure 1; Table 1).[67,86,87] We attempted to concentrate our low concentrations through fractional distillation to partial success but not presently sufficient for scale up (Figure S10). The direct conversion of glycolaldehyde alone to sugars is another avenue enabled by the formose reaction, as glycolaldehyde alone enables sugar generation (Figure S8). However, presently achievable e-CO_2Glyc concentration is too low (~60 μM) to alone support the formose reaction (Figure S11). A concentration of at least ~10 mM glycolaldehyde is required for sugar generation through the formose reaction (Figure S12). As a path to formaldehyde in high titers from CO_2 is within industrial capacity (Table 1), we focused our efforts on confirming the role e-CO_2Glyc as the essential formose autocatalyst with commercially available formaldehyde used as a stand-in. Hence, we demonstrate a proof-of-concept sugar generation from commercial formaldehyde (to be CO_2-derived) autocatalyzed by e-CO_2Glyc in a chemically complex medium.

We used the unadulterated CO_2 electrolysis product stream as the glycolaldehyde source with our optimized formose reaction conditions for the conversion of formaldehyde to sugars. The high $KHCO_3$ concentration (0.1 M) in the electrolysis product mixture posed further obstacles. First, the Ca^{2+} and CO_3^{2-} combine to form highly insoluble $CaCO_3$ which does not adequately catalyze the formose reaction. Second, $KHCO_3$ acts as a buffer that alters the optimal pH upon addition of the divalent metal catalyst. Third, the high salinity of the reaction mixture complicates product characterization with mass spectrometry by suppressing ionization. Nonetheless, we were able to introduce sufficient $Ca(OH)_2$ for the reaction to proceed by adding excess $Ca(OH)_2$ 10 mM above the concentration of $KHCO_3$ and by carefully titrating the reaction mixture pH with NaOH/HCl to pH 11.

The use of the unadulterated CO_2 electrolysis product stream to generate CO_2RR-autocatalyzed sugars (CO_2Sugars) presents another challenge with the introduction of a multitude of coexisting CO_2-derived molecules. The complexity of the reaction mixture complicates the analysis of CO_2Sugars. Therefore, unlike in the previous formose reaction optimizations, HPAEC-PAD measurements are in part affected by the high concentrations of other CO_2-derived products (e.g., ethanol, $HCOO^-$) and by the presence of HCO_3^- anions (Figure S13). Fortunately, the spectral signature of sugars is easily distinguishable using ^{1}H-NMR. Specifically, the chemical shifts for

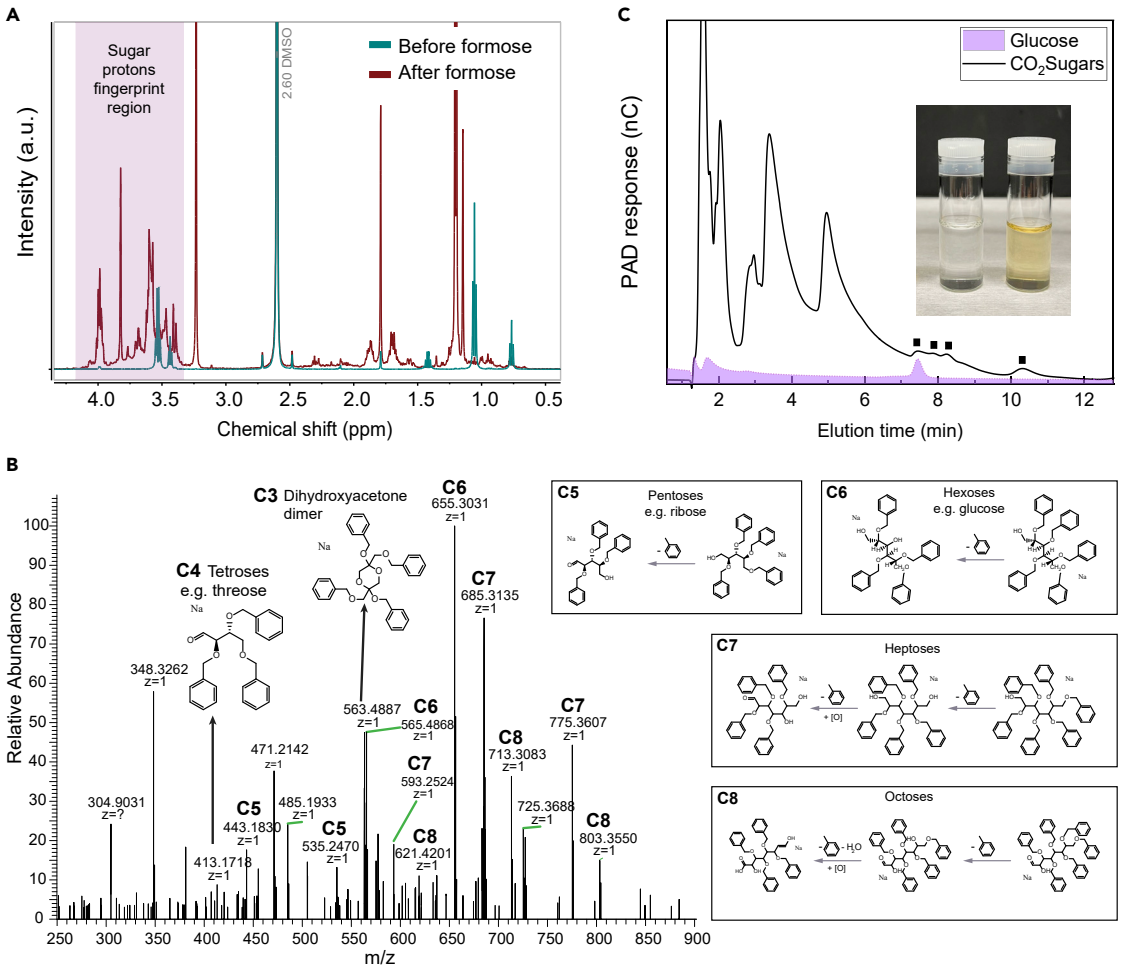

Figure 4. Sugar synthesis catalyzed by CO_2-derived glycolaldehyde

(A) ^{1}H-NMR spectra pre- and post-formose reaction demonstrating the appearance of carbohydrate protons in the 3.5–5 ppm region.

(B) ESI-MS spectrum reveals a diverse mixture of benzylated sugars including pentoses, hexoses, heptoses, and octoses.

(C) HPAEC-PAD spectrum reveals the presence of distinguishable CO_2Sugars obtained from the product stream of Cu NP ensemble at −0.80 V versus RHE. Visible peaks in the chromatograms are indicated by black squares. One of them is identified as glucose as it overlays closely with the glucose reference chromatogram. Inset picture displays the product of the formose reaction without e-CO_2Glyc (left) and autocatalyzed by e-CO_2Glyc (right). The yellow color is characteristic of sugar production.

carbohydrate protons are typically observed in the 3.5–5 ppm region, whereas most of the other CO_2RR products are found in the 0–4 and >7 ppm region (Figure S14). Therefore, the appearance of multiple peaks in this region was used as an initial indication for the formation of CO_2Sugars. With the Ca^{2+} catalyst concentration and pH optimization, ^{1}H-NMR results indicate that sugar formation can be autocatalyzed by e-CO_2Glyc (Figure 4A).

Beyond the sugar fingerprint identified by ^{1}H-NMR, we used electrospray ionization mass spectrometry (ESI-MS) to further determine the variety of CO_2Sugars.[88] As previously mentioned, the high salinity of our reaction containing K^+, Na^+, and Ca^{2+} poses an obstacle to ESI-MS analysis. Therefore, we separated our CO_2Sugars from the salty aqueous solution via liquid-liquid extraction by protecting their hydroxyl groups (benzylation), thus increasing their solubility in organic solvents (Figure S15).[89] The derivatization of CO_2Sugars by benzylation and separation from the

salty mixture allowed their characterization by ESI-MS. These measurements revealed a diverse mixture of fully and partially benzylated carbohydrates ranging from three to eight carbons (Figure 4B).

Although powerful, ESI-MS analysis is limited to the identification of sugars of the same molecular weight. HPAEC-PAD remains the method of choice to distinguish multiple carbohydrates of similar compositions (i.e., glucose from galactose or fructose). The high baseline tailing effect observed in the chromatogram of CO_2Sugars likely results from the saturation of the column due to the high concentrations of HCO_3^- present as buffer (Figure S13). Nevertheless, carbohydrates in the reaction mixture are still distinguishable during HPAEC-PAD measurements. Comparing the chromatograms of carbohydrate standards with the reaction mixture of CO_2Sugars confirms the presence of biologically relevant sugars such as glucose (Figure 4C). Further separation of the reaction mixture from HCO_3^- and other overlapping molecules will be required to improve the analysis of CO_2Sugars and enable quantification by HPAEC-PAD. Additionally, a more extensive survey of carbohydrate standards beyond those that are significant as biological feedstocks should be performed to complete the catalog of CO_2Sugars produced.

To highlight the broad applicability and reproducibility of employing e-CO_2Glyc as the autocatalyst in the formose reaction, we used e-CO_2Glyc obtained at varying CO_2RR conditions. We compared the e-CO_2Glyc generated at three successive potentials with the Cu NP ensemble and with Cu foil. The input e-CO_2Glyc concentration was normalized across the electrolytes before beginning the formose reaction. As demonstrated by the ^{1}H-NMR and HPAEC-PAD spectra (Figures S16 and S17) for the four different conditions, there is little difference in the ensuing CO_2Sugars. This confirms that the formose reaction is robustly adaptive to different CO_2RR conditions, given sufficient e-CO_2Glyc.

Bacterial culture supported by CO_2Sugars

With biologically relevant sugars—ribose, galactose, fructose, arabinose, and glucose—in hand, we sought to use them to sustain bacterial growth. Glucose is the preferred feedstock for *E. coli*; however, it can also metabolize a variety of other carbohydrates including many of those produced in the formose reaction.[90] We collected the products from the standard formose reaction and from CO_2Sugars and employed them directly as feed sources for *E. coli* cultures. We used minimal processing to prepare the formose sugars; briefly, we syringe filtered the solutions directly after the formose reaction to remove precipitates, crystallized the sugars via rotary evaporation which also removed cytotoxic components (e.g., CH_3OH, ethanol), and added a commensurate amount (0.1% w/v) to M9 minimal bacterial medium (Table S2). The medium containing the formose sugars was syringe sterilized before inoculating with *E. coli*. Culture growth and biomass accumulation were assessed by optical density measurements. Formose- and CO_2Sugars-fed cultures achieved maximum optical densities of ~0.262 and ~0.223, reaching stationary phases after 4.3 and 3.8 h, respectively (Figure 5A). In comparison, the optical density of a control *E. coli* culture provided with 0.1% pure glucose was ~0.588 (Figure S18). The optical density of the formose-fed *E. coli* culture is expectedly lower as the feed source consists of a mixture of sugar isomers that may not be metabolizable or metabolized sub-optimally when compared with pure D-glucose. Garcia Martinez et al. estimate the caloric content of formose sugars to be 1.39 kcal/g, whereas the caloric content of glucose is 4 kcal/g.[7] Interestingly, the ratio of glucose calories to formose sugar calories is similar to the ratio of cell densities between glucose- and CO_2Sugar-fed *E. coli* cultures, at 2.88 and 2.64, respectively. These results

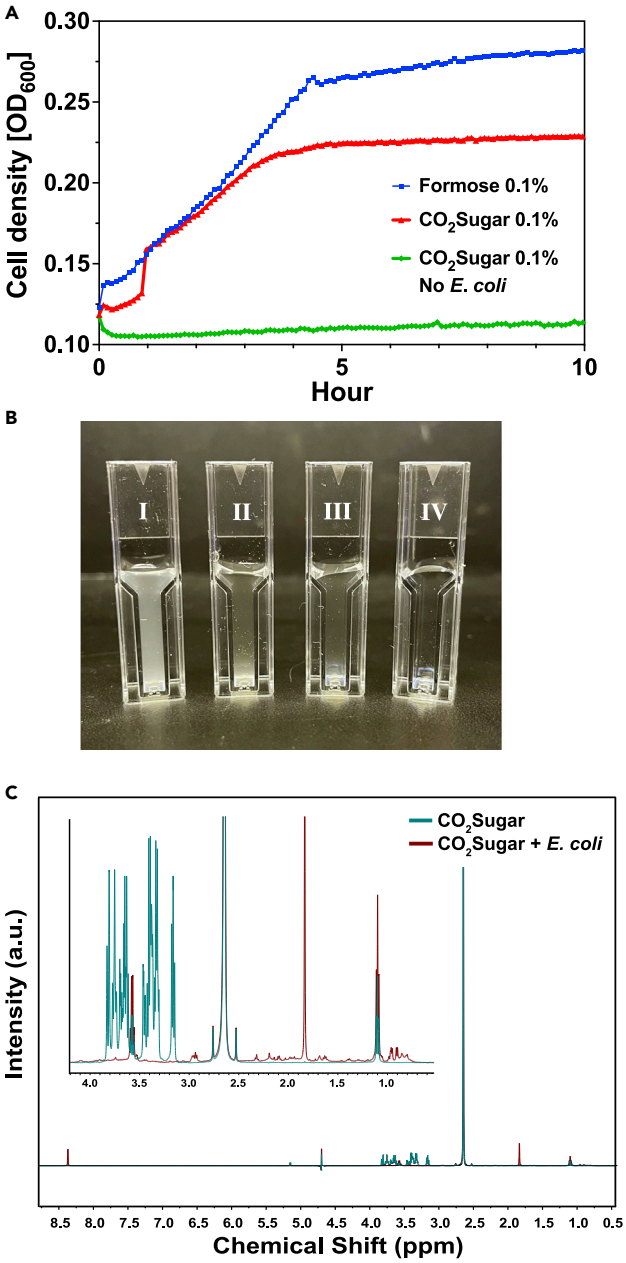

Figure 5. Utilization of CO_2Sugar as a bacterial feedstock

(A) Optical density measurements of *Escherichia coli* (*E. coli*) cultured with formose sugars (blue) and CO_2Sugars (red). Control is CO_2Sugars without *E. coli* (green).

(B) Picture comparing the visual differences between *E. coli* cultures provided with different sugars. From left to right: I, glucose; II, formose sugars; III, CO_2Sugars; and IV, CO_2Sugars without *E. coli*.

(C) ^{1}H-NMR spectra of CO_2Sugar containing minimal medium pre- and post-*E. coli* culture growth. Inset shows magnified 1–4 ppm region.

demonstrate that CO_2Sugars can sustain heterotrophic microorganisms in a raw form with little processing. The minimization of processing and separation steps is especially valuable for industrial and extra-terrestrial applications. Furthermore, we verified that available CO_2Sugars present in minimal medium were consumed during bacterial growth. To establish this, we obtained ^{1}H-NMR spectra of the

CO_2Sugars-supplemented minimal medium before and after the culturing period. As exhibited in Figure 5C, the carbohydrate associated proton peaks mostly disappear after bacteria are grown in the medium. Additionally, the appearance of a peak at ~1.8 ppm indicates the formation of acetate during culture growth. *E. coli* secrete acetate as a by-product of glycolysis during aerobic growth in minimal medium.[29] Finally, *E. coli* growth can be visually confirmed in the medium containing different sugars sources (Figure 5B). In the future, we envision the production of CO_2Sugars could be coupled with a biomanufacturing platform to generate value-added products on demand.

When taken together, we demonstrate an approach to employ the outputs of CO_2 electrosynthesis to generate sugars. Our work invites the CO_2 electrocatalysis community to reconsider the processing value of so far overlooked byproducts. Although minor, some of the building blocks present in the streamline of CO_2 electrolysis could be readily utilized for the construction of biologically significant molecules. However, there remain several scale-up steps to be determined before achieving a catalytic turnover akin to biological processes. The electrochemical production of both glycolaldehyde and formaldehyde presented in our work is limited to the μM scale. To maximize these turnovers, catalyst development, electrochemical conditions, and reactors will require further investigation. As an example, the application of a flow cell design can be used to minimize the further reduction of the produced aldehydes, or it could facilitate a two-step CO_2RR process. Further studies of the catalyst properties necessary to advance the CO_2 electroreduction to formaldehyde will be required to achieve the targeted activity. For the maximization of both aldehyde concentrations, an additional processing step of distillation should be considered. With such developments, we envision that this inorganic platform could rival photosynthesis in commercial sugar production and could mitigate CO_2-driven climate change. Overall, this proof of concept demonstrates how various catalytic systems can be tailored to facilitate CO_2 conversion to life-sustaining molecules, far beyond the hydrocarbons usually reported in the field of CO_2 electrocatalytic upcycling.

EXPERIMENTAL PROCEDURES

Resource availability

Lead contact

Further information and requests for resources should be directed to the lead contact, Dr. Peidong Yang (p_yang@berkeley.edu).

Materials availability

This study did not generate new unique reagents and all chemicals were purchased from commercial resources and used as received.

Data and code availability

The datasets generated in this study are available from the lead contact on reasonable request.

Methods

Electrochemical CO_2 reduction

7 nm Cu NPs were synthesized as previously reported.[35] BDD electrode (Electrode Kit Boron Doped Diamond, IKA) was rinsed with 20% HNO_3 and sonicated in DI water before use. All electrochemical measurements were carried in a custom-made H-cell consisting of two main compartments separated by a Selemion AMV anion exchange membrane (AEM). Ag/AgCl (WPI, 3 M KCl) was used as a reference electrode, and a platinum wire was used as a counter electrode.

For glycolaldehyde production, 0.1 M $KHCO_3$ electrolyte was prepared by purging a 0.05 M K_2CO_3 (99.997% trace metal basis) solution with CO_2 overnight. Both the working and counter chambers were filled with 17 mL of the electrolyte and vigorous stirring was maintained in the working chamber. The input stream of CO_2 was humidified by bubbling through deionized (DI) water before being introduced into the cell. Before each measurement, the 17 mL catholyte was purged with 20 sccm CO_2 for 15–20 min until saturated.

Formaldehyde production was carried in various electrolytes including 0.1 M NaCl, 0.1 M $KHCO_3$, and 0.1 M $HClO_4$. The same procedure as for the CO_2-to-glycolaldehyde reaction described above was executed.

All electrode potentials measured against 3 M KCl Ag/AgCl reference were converted to the RHE scale using E (versus RHE) = E (versus Ag/AgCl) + 0.210 V + 0.0591 × pH. For all electrochemical experiments, 84% of ohmic loss was compensated by the potentiostat (Biologic) in real time and the remaining 16% was manually post-corrected. Glycolaldehyde concentration was determined using quantitative NMR (qNMR) (Bruker AV-600).

The concentration of gases produced throughout electrolysis was measured using a gas chromatograph (SRI GC) connected at the outlet of the cell. Gas chromatograph is equipped with a molecular sieve 13X (1/8″ × 6′) and hayesep D (1/8″ × 6′) column with Ar flowing as a carrier gas. Sample for GC was collected at 20-min intervals and the separated gas products were analyzed by a thermal conductivity detector (for H_2) and a flame ionization detector (for CO and hydrocarbons). Quantification of the products was performed with conversion factors derived from the standard calibration gases and the concentration of gas measured was further converted to partial current density.

A formaldehyde detection assay (Sigma-Aldrich MAK131) was employed to quantify formaldehyde concentrations. Briefly, formaldehyde is derivatized with acetoacetanilide in the presence of ammonia yielding a fluorescent product with excitation and emission wavelengths at 370 and 470 nm, respectively. The fluorescent signal proportional to formaldehyde concentration was read using a Biotek Synergy LX Multi-Mode microplate reader.

FEs were calculated from the amount of charge passed to produce each product divided by the total charge passed at a specific time (gas) or during the overall run (liquid).

Formose reaction

The formose reaction was performed as described in previous literature.[77,79] Initial reagents were paraformaldehyde, glycolaldehyde dimer, and $Ca(OH)_2$ (Sigma Aldrich). Commercial paraformaldehyde was suspended in DI water, heated to 70°C, and refluxed under alkaline conditions to depolymerize, producing a homogeneous, colorless solution. Glycolaldehyde and $Ca(OH)_2$ were dissolved in DI water. The total reaction volume was typically 3 mL with 10 mM $Ca(OH)_2$, with the concentrations of formaldehyde and glycolaldehyde as well as the temperature dependent on desired experimental conditions. The reactions were carried out for 75 min and then quickly cooled down to room temperature. Upon completion, the samples exhibited the characteristic bright yellow color of the formose reaction. For CO_2-derived formose reaction, the CO_2RR electrolyte was used directly without any processing. For example, for a 3 mL reaction volume, 1.5 mL of CO_2RR electrolyte with

30 μM glycolaldehyde was combined with an equivalent volume of DI water. $Ca(OH)_2$ and formaldehyde were added to concentrations of 60 and 70 mM, respectively. The reaction was maintained at 75°C for 75 min. The pH was titrated with 1 M NaOH/HCl to 11.

Product and material characterization

^{1}H-NMR. The liquid products accumulated during CO_2 electrolysis, and the sugars produced during the formose reaction are analyzed by qNMR (Bruker AV-600) following the same procedure. Dimethyl sulfoxide is used as an internal standard and an aliquot of the solution of interest prepared in D_2O. Solvent presaturation technique is implemented to suppress the water peak.

Mass spectrometry. The produced carbohydrates are benzylated to ensure their separation from their salty matrix post-formose reaction.[89] The aqueous sample is mixed with NaOH/K_2CO_3 (1/4, w/w), benzene, isopropanol, tetrabutylammonium hydrogen sulfate, benzyl chloride, and DMSO. The solution is then vigorously stirred using a stir bar at room temperature for 4 h. Subsequently, the mixture is worked up using cyclohexane, washed with water, and dried over Na_2SO_4. The benzylated carbohydrates were then injected into an electrospray ionization mass spectrometer for mass analysis.

HPAEC-PAD. The completed reactions were analyzed by HPAEC-PAD on a Dionex ICS-5000. The samples were run on a CarboPac PA20 IC column using a 0.4 mL/min isocratic gradient as follows: with 10 mM NaOH for 30 min, 100 mM NaOH for 5 min, and 10 mM NaOH for 5 min. A gold electrode in carbohydrate quad potential mode was employed as the detector. Upon injection, the elution is carried with 10 mM NaOH for 30 min, 100 mM NaOH for 5 min, and 10 mM NaOH for 5 min. Runs were compared with standards of (2 to 6 carbons) biologically relevant sugars: arabinose, glucose, ribose, fructose, acetaldehyde, and formaldehyde were employed to identify peaks in the trace.

SEM. Cu NP coated and BDD electrodes were directly imaged by SEM at 5 keV (Ultra 55-FESEM).

Cell culture

XL1-blue *E. coli* cells were obtained from the Berkeley-QB3 MacroLab. *E. coli* stock stored at −80°C, was inoculated in lysogeny broth (Table S1), and incubated at 37°C in three consecutive cultures to remove any cryoprotectant. The formose reaction solution was filtered to remove precipitates, and the products were recovered using a rotary evaporator. The experiment appropriate mass of bulk formose sugars (0%–0.1% [w/v]) was added to the M9 minimal medium and syringe filtered to sterilize. The cells were then inoculated in M9 minimal medium (Table S2) supplemented with glucose or formose sugars. *E. coli* growth curves were acquired in a Tecan M1000 plate reader in a 48-well plate for 12 h at 37°C.

SUPPLEMENTAL INFORMATION

Supplemental information can be found online at https://doi.org/10.1016/j.joule.2022.08.007.

ACKNOWLEDGMENTS

This work was supported by an award from the National Aeronautics and Space Administration (NASA) under the Centennial Challenges competition program. The authors thank the judges and competition administrators for their feedback.

This work was also supported by the Director, Office of Science, Office of Basic Energy Sciences, Chemical Sciences, Geosciences, & Biosciences Division of the US Department of Energy under contract DE-AC02-05CH11231, FWP CH030201 (Catalysis Research Program) and by NASA, under grant number NNX17AJ31G. ICP-OES was supported by the Microanalytical Facility, College of Chemistry, UC Berkeley. We thank the staff at UC Berkeley's NMR facility in the College of Chemistry (CoC-NMR) for spectroscopic assistance. Instruments in the CoC-NMR are supported in part by the National Institues of Health under grant number S10OD024998. We also thank Z. Zhou at the QB3 Chemistry Mass Spectrometry Facility for her assistance with GC-MS measurements. SEM was conducted using facilities at the National Center for Electron Microscopy and Imaging and Nanofabrication facilities at the Molecular Foundry. Work at the Molecular Foundry was supported by the Office of Science, Office of Basic Energy Sciences, of the US Department of Energy under contract DE-AC02-05CH11231. We also thank Dr. Kyle Sander for assistance with *E. coli* growth experiments. S.C.-B. thanks the Philomathia Foundation for a personal fellowship.

AUTHOR CONTRIBUTIONS

S.C.-B. and S.L. contributed equally and have the right to list their name first in relevant applications. S.C.-B. and S.L. designed and led the experiments. S.C.-B., M.B.R., Y.L., and P.Y. conceived of the project. Y.L. assisted in CO_2 reduction experiments. T.C.D. helped with HPAEC-PAD work. J.N.C.S. and D.K.N. facilitated MS protocol development. All authors wrote, discussed, and revised the manuscript.

DECLARATION OF INTERESTS

The authors declare no competing interests.

Received: March 18, 2022
Revised: June 28, 2022
Accepted: August 17, 2022
Published: September 19, 2022

REFERENCES

1. Liu, Q., Wu, L., Jackstell, R., and Beller, M. (2015). Using carbon dioxide as a building block in organic synthesis. Nat. Commun. *6*, 5933.

2. Goeppert, A., Czaun, M., Surya Prakash, G.K., and Olah, G.A. (2012). Air as the renewable carbon source of the future: an overview of CO_2 capture from the atmosphere. Energy Environ. Sci. *5*, 7833–7853.

3. Hepburn, C., Adlen, E., Beddington, J., Carter, E.A., Fuss, S., Mac Dowell, N., Minx, J.C., Smith, P., and Williams, C.K. (2019). The technological and economic prospects for CO_2 utilization and removal. Nature *575*, 87–97.

4. Manning, C.V., McKay, C.P., and Zahnle, K.J. (2006). Thick and thin models of the evolution of carbon dioxide on Mars. Icarus *180*, 38–59.

5. Muscatello, A.C., and Santiago-Maldonado, E. (2012). Mars in situ resource utilization technology evaluation. https://ntrs.nasa.gov/api/citations/20120001775/downloads/20120001775.pdf.

6. Berliner, A.J., Hilzinger, J.M., Abel, A.J., McNulty, M.J., Makrygiorgos, G., Averesch, N.J.H., Sen Gupta, S., Benvenuti, A., Caddell, D.F., Cestellos-Blanco, S., et al. (2021). Towards a biomanufactory on Mars. Front. Astron. Space Sci. *8*, 120.

7. García Martínez, J.B., Alvarado, K.A., Christodoulou, X., and Denkenberger, D.C. (2021). Chemical synthesis of food from CO_2 for space missions and food resilience. J. CO_2 Util. *53*, 101726.

8. Mac Dowell, N., Fennell, P.S., Shah, N., and Maitland, G.C. (2017). The role of CO_2 capture and utilization in mitigating climate change. Nat. Clim. Change *7*, 243–249.

9. Jiang, Z., Xiao, T., Kuznetsov, V.L., and Edwards, P.P. (2010). Turning carbon dioxide into fuel. Philos. Trans. A Math. Phys. Eng. Sci. *368*, 3343–3364.

10. Oloman, C., and Li, H. (2008). Electrochemical processing of carbon dioxide. ChemSusChem *1*, 385–391.

11. Feaster, J.T., Shi, C., Cave, E.R., Hatsukade, T., Abram, D.N., Kuhl, K.P., Hahn, C., Nørskov, J.K., and Jaramillo, T.F. (2017). Understanding selectivity for the electrochemical reduction of carbon dioxide to formic acid and carbon monoxide on metal electrodes. ACS Catal. *7*, 4822–4827.

12. Philips, M.F., Gruter, G.-J.M., Koper, M.T.M., and Schouten, K.J.P. (2020). Optimizing the electrochemical reduction of CO_2 to formate: a state-of-the-art analysis. ACS Sustainable Chem. Eng. *8*, 15430–15444.

13. Hori, Y., Kikuchi, K., and Suzuki, S. (1985). Production of CO and CH_4 in electrochemical reduction of CO_2 at metal electrodes in aqueous hydrogencarbonate solution. Chem. Lett. 1695–1698.

14. Jitaru, M., Lowy, D.A., Toma, M., Toma, B.C., and Oniciu, L. (1997). Electrochemical reduction of carbon dioxide on flat metallic cathodes. J. Appl. Electrochem. *27*, 875–889.

15. Zheng, Y., Vasileff, A., Zhou, X., Jiao, Y., Jaroniec, M., and Qiao, S.-Z. (2019). Understanding the roadmap for electrochemical reduction of CO2 to multi-carbon oxygenates and hydrocarbons on copper-based catalysts. J. Am. Chem. Soc. *141*, 7646–7659.

16. Ross, M.B., de Luna, P., Li, Y., Dinh, C.T., Kim, D., Yang, P., and Sargent, E.H. (2019). Designing materials for electrochemical carbon dioxide recycling. Nat. Catal. *2*, 648–658.

17. Xue, Y., Guo, Y., Cui, H., and Zhou, Z. (2021). Catalyst design for electrochemical reduction of CO_2 to multicarbon products. Small Methods *5*, e2100736.

18. Kuhl, K.P., Cave, E.R., Abram, D.N., and Jaramillo, T.F. (2012). New insights into the electrochemical reduction of carbon dioxide on metallic copper surfaces. Energy Environ. Sci. *5*, 7050–7059.

19. Ting, L.R.L., García-Muelas, R., Martín, A.J., Veenstra, F.L.P., Chen, S.T., Peng, Y., Per, E.Y.X., Pablo-García, S., López, N., Pérez-Ramírez, J., and Yeo, B.S. (2020). Electrochemical reduction of carbon dioxide to 1-butanol on oxide-derived copper. Angew. Chem. Int. Ed. Engl. *132*, 21258–21265.

20. Chen, H., Dong, F., and Minteer, S.D. (2020). The progress and outlook of bioelectrocatalysis for the production of chemicals, fuels and materials. Nat. Catal. *3*, 225–244.

21. Cestellos-Blanco, S., Zhang, H., Kim, J.M., Shen, Y.x., and Yang, P. (2020). Photosynthetic semiconductor biohybrids for solar-driven biocatalysis. Nat. Catal. *3*, 245–255.

22. Jourdin, L., and Burdyny, T. (2021). Microbial electrosynthesis: where do we go from here? Trends Biotechnol. *39*, 359–369.

23. Salimijazi, F., Kim, J., Schmitz, A.M., Grenville, R., Bocarsly, A., and Barstow, B. (2020). Constraints on the efficiency of engineered electromicrobial production. Joule *4*, 2101–2130.

24. Li, H., Opgenorth, P.H., Wernick, D.G., Rogers, S., Wu, T.Y., Higashide, W., Malati, P., Huo, Y.X., Cho, K.M., and Liao, J.C. (2012). Integrated electromicrobial conversion of CO2to higher alcohols. Science *335*, 1596.

25. Haas, T., Krause, R., Weber, R., Demler, M., and Schmid, G. (2018). Technical photosynthesis involving CO_2 electrolysis and fermentation. Nat. Catal. *1*, 32–39.

26. Hegner, R., Rosa, L.F.M., and Harnisch, F. (2018). Electrochemical CO_2 reduction to formate at indium electrodes with high efficiency and selectivity in pH neutral electrolytes. Appl. Cat. B *238*, 546–556.

27. Zheng, T., Zhang, M., Wu, L., Guo, S., Liu, X., Zhao, J., Xue, W., Li, J., Liu, C., Li, X., et al. (2022). Upcycling CO_2 into energy-rich long-chain compounds via electrochemical and metabolic engineering. Nat. Catal. *5*, 388–396.

28. Abel, A.J., Adams, J.D., and Clark, D.S. (2022). A comparative life cycle analysis of electromicrobial production systems. Energy Environ. Sci. *9*, 3062–3085.

29. Pinhal, S., Ropers, D., Geiselmann, J., and de Jong, H. (2019). Acetate metabolism and the inhibition of bacterial growth by acetate. J. Bacteriol. *201*. e00147-19.

30. Kandler, O. (1983). Carbohydrate metabolism in lactic acid bacteria. Antonie Leeuwenhoek *49*, 209–224.

31. Cheng, M.H., Huang, H., Dien, B.S., and Singh, V. (2019). The costs of sugar production from different feedstocks and processing technologies. Biofuels Bioprod. Biorefin. *13*, 723–739.

32. Cummings, J.H., Roberfroid, M.B., Andersson, H., Barth, C., Ferro-Luzzi, A., Ghoos, Y., Gibney, M., Hermansen, K., James, W.P.T., Korver, O., et al. (1997). A new look at dietary carbohydrate: chemistry, physiology and health. Paris Carbohydrate Group. Eur. J. Clin. Nutr. *51*, 417–423.

33. Cai, T., Sun, H., Qiao, J., Zhu, L., Zhang, F., Zhang, J., Tang, Z., Wei, X., Yang, J., Yuan, Q., et al. (2021). Cell-free chemoenzymatic starch synthesis from carbon dioxide. Science *373*, 1523–1527.

34. Harbaugh, J. (2021). NASA awards $750,000 in competition to convert CO2 into sugar. https://www.nasa.gov/directorates/spacetech/centennial_challenges/75K-awarded-in-competition-to-convert-carbon-dioxide-into-sugar.html.

35. Kim, D., Kley, C.S., Li, Y., and Yang, P. (2017). Copper nanoparticle ensembles for selective electroreduction of CO_2 to C_2–C_3 products. Proc. Natl. Acad. Sci. USA *114*, 10560–10565.

36. Li, Y., Kim, D., Louisia, S., Xie, C., Kong, Q., Yu, S., Lin, T., Aloni, S., Fakra, S.C., and Yang, P. (2020). Electrochemically scrambled nanocrystals are catalytically active for CO2-to-multicarbons. Proc. Natl. Acad. Sci. USA *117*, 9194–9201.

37. Mohan, D., Pittman, C.U., Jr., and Steele, P.H. (2006). Pyrolysis of wood/biomass for bio-oil: a critical review. Energy Fuels *20*, 848–889.

38. Schandel, C.B., Høj, M., Osmundsen, C.M., Jensen, A.D., and Taarning, E. (2020). Thermal cracking of sugars for the production of glycolaldehyde and other small oxygenates. ChemSusChem *13*, 688–692.

39. Nakata, K., Ozaki, T., Terashima, C., Fujishima, A., and Einaga, Y. (2014). High-yield electrochemical production of formaldehyde from CO_2 and seawater. Angew. Chem. Int. Ed. Engl. *53*, 871–874.

40. Lee, D.-K., Kim, D.-S., and Kim, S.-W. (2001). Selective formation of formaldehyde from carbon dioxide and hydrogen over PtCu/SiO_2. Appl. Organomet. Chem. *15*, 148–150.

41. Daza, Y.A., and Kuhn, J.N. (2016). CO_2 conversion by reverse water gas shift catalysis: comparison of catalysts, mechanisms and their consequences for CO_2 conversion to liquid fuels. RSC Adv. *6*, 49675–49691.

42. Bhargava, S.S., Proietto, F., Azmoodeh, D., Cofell, E.R., Henckel, D.A., Verma, S., Brooks, C.J., Gewirth, A.A., and Kenis, P.J.A. (2020). System design rules for intensifying the electrochemical reduction of CO_2 to CO on Ag nanoparticles. ChemElectroChem *7*, 2001–2011.

43. Bahmanpour, A.M., Hoadley, A., and Tanksale, A. (2015). Formaldehyde production via hydrogenation of carbon monoxide in the aqueous phase. Green Chem. *17*, 3500–3507.

44. Yao, L., Pan, Y., Shen, X., Wu, D., Bentalib, A., and Peng, Z. (2020). Utilizing hydrogen underpotential deposition in CO reduction for highly selective formaldehyde production under ambient conditions. Green Chem. *22*, 5639–5647.

45. Herman, R.G., Klier, K., Simmons, G.W., Finn, B.P., Bulko, J.B., and Kobylinski, T.P. (1979). Catalytic synthesis of methanol from COH_2: I. Phase composition, electronic properties, and activities of the Cu/ZnO/M_2O_3 catalysts. J. Cat *56*, 407–429.

46. Boutin, E., Wang, M., Lin, J.C., Mesnage, M., Mendoza, D., Lassalle-Kaiser, B., Hahn, C., Jaramillo, T.F., and Robert, M. (2019). Aqueous electrochemical reduction of carbon dioxide and carbon monoxide into methanol with cobalt phthalocyanine. Angew. Chem. Int. Ed. Engl. *58*, 16172–16176.

47. Choi, E.G., Song, K.H., An, S.R., Lee, K.Y., Youn, M.H., Park, K.T., Jeong, S.K., and Kim, H.J. (2018). Cu/ZnO/AlOOH catalyst for methanol synthesis through CO_2 hydrogenation. Korean J. Chem. Eng. *35*, 73–81.

48. Yang, D., Zhu, Q., Chen, C., Liu, H., Liu, Z., Zhao, Z., Zhang, X., Liu, S., and Han, B. (2019). Selective electroreduction of carbon dioxide to methanol on copper selenide nanocatalysts. Nat. Commun. *10*, 677.

49. Sperber, H. (1969). Herstellung von formaldehyd aus methanol in der BASF. Chemie Ing. Techn. *41*, 962–966.

50. Bahmanpour, A.M., Hoadley, A., and Tanksale, A. (2014). Critical review and exergy analysis of formaldehyde production processes. Rev. Chem. Eng. *30*, 583–604.

51. Korzeniewski, C., and Childers, C.L. (1998). Formaldehyde yields from methanol electrochemical oxidation on platinum. J. Phys. Chem. B *102*, 489–492.

52. Dinger, F., and Platt, U. (2020). Towards an artificial carbohydrates supply on earth. Front. Sustain. Food Syst. *4*, 90.

53. Deng, J., Pan, T., Xu, Q., Chen, M.Y., Zhang, Y., Guo, Q.X., and Fu, Y. (2013). Linked strategy for the production of fuels via formose reaction. Sci. Rep. *3*, 1244.

54. Alston, J.M., Sumner, D.A., and Vosti, S.A. (2008). Farm subsidies and obesity in the United States: national evidence and international comparisons. Food Policy *33*, 470–479.

55. Benson, P. (2008). EL CAMPO: faciality and structural violence in farm labor camps. Cult. Anthropol. *23*, 589–629.

56. Zhong, H., Feng, K., Sun, L., Tian, Z., Fischer, G., Cheng, L., and Munoz Castillo, R. (2021). Water-land tradeoffs to meet future demands for sugar crops in Latin America and the Caribbean: a bio-physical and socio-economic nexus perspective. Resour. Conserv. Recy. *169*, 105510.

57. Landis, A.E., Miller, S.A., and Theis, T.L. (2007). Life cycle of the corn-soybean agroecosystem for biobased production. Environ. Sci. Technol. *41*, 1457–1464.

58. Korchak, M., Yermakov, S., Maisus, V., Oleksiyko, S., Pukas, V., and Zavadskaya, I. (2020). Problems of field contamination when growing energy corn as monoculture. E3S Web Conf. *154*, 01009.

59. Bracher, P.J. (2015). Origin of life: primordial soup that cooks itself. Nat. Chem. *7*, 273–274.

60. Breslow, R. (1959). On the mechanism of the formose reaction. Tetrahedron Lett. *1*, 22–26.

61. Eckhardt, A.K., Linden, M.M., Wende, R.C., Bernhardt, B., and Schreiner, P.R. (2018). Gas-phase sugar formation using hydroxymethylene as the reactive formaldehyde isomer. Nat. Chem. *10*, 1141–1147.

62. Delidovich, I.V., Simonov, A.N., Taran, O.P., and Parmon, V.N. (2014). Catalytic formation of monosaccharides: from the formose reaction towards selective synthesis. ChemSusChem *7*, 1833–1846.

63. Robinson, W.E., Daines, E., van Duppen, P., de Jong, T., and Huck, W.T.S. (2022). Environmental conditions drive self-organization of reaction pathways in a prebiotic reaction network. Nat. Chem. *14*, 623–631.

64. Nguyen, T.N., and Dinh, C.T. (2020). Gas diffusion electrode design for electrochemical carbon dioxide reduction. Chem. Soc. Rev. *49*, 7488–7504.

65. Marcos-Madrazo, A., Casado-Coterillo, C., and Irabien, Á. (2019). Sustainable membrane-coated electrodes for CO_2 electroreduction to methanol in alkaline media. ChemElectroChem *6*, 5273–5282.

66. Liu, Y., Li, F., Zhang, X., and Ji, X. (2020). Recent progress on electrochemical reduction of CO_2 to methanol. Curr. Opin. Green Sustain. Chem. *23*, 10–17.

67. Heim, L.E., Konnerth, H., and Prechtl, M.H.G. (2017). Future perspectives for formaldehyde: pathways for reductive synthesis and energy storage. Green Chem. *19*, 2347–2355.

68. Thrane, J., Mentzel, U.V.v., Thorhauge, M., Høj, M., and Jensen, A.D. (2021). A review and experimental revisit of alternative catalysts for selective oxidation of methanol to formaldehyde. Catalysts *11*, 1329.

69. Gerberich, H.R., and Seaman, G.C. (2004). Formaldehyde. Kirk-Othmer Encyclopedia of Chemical Technology (John Wiley & Sons).

70. Bersier, P.M., Carlsson, L., and Bersier, J. (1994). Electrochemistry for a better environment. Topics in Current Chemistry, 113–229.

71. Charnay, B.P., Cui, Z., Marx, M.A., Palazzo, J., and Co, A.C. (2021). Insights into the CO_2 reduction pathway through the electrolysis of aldehydes on copper. ACS Cat. *11*, 3867–3876.

72. Clark, E.L., and Bell, A.T. (2018). Direct observation of the local reaction environment during the electrochemical reduction of CO_2. J. Am. Chem. Soc. *140*, 7012–7020.

73. Löffler, M., Khanipour, P., Kulyk, N., Mayrhofer, K.J.J., and Katsounaros, I. (2020). Insights into liquid product formation during carbon dioxide reduction on copper and oxide-derived copper from quantitative real-time measurements. ACS Catal. *10*, 6735–6740.

74. Birdja, Y.Y., and Koper, M.T.M. (2017). The importance of Cannizzaro-type reactions during electrocatalytic reduction of carbon dioxide. J. Am. Chem. Soc. *139*, 2030–2034.

75. Mizuno, T., and Weiss, A.H. (1974). Synthesis and utilization of formose sugars. Adv. Carbohydr. Chem. Biochem. *29*, 173–227.

76. Butlerow, A. (1861). Bildung einer zuckerartigen substanz durch synthese. Ann. Chem. Pharm. *120*, 295–298.

77. Lambert, J.B., Gurusamy-Thangavelu, S.A., and Ma, K. (2010). The silicate-mediated formose reaction: bottom-up synthesis of sugar silicates. Science *327*, 984–986.

78. Pallmann, S., Šteflová, J., Haas, M., Lamour, S., Henß, A., and Trapp, O. (2018). Schreibersite: an effective catalyst in the formose reaction network. New J. Phys. *20*, 55003.

79. Appayee, C., and Breslow, R. (2014). Deuterium studies reveal a new mechanism for the formose reaction involving hydride shifts. J. Am. Chem. Soc. *136*, 3720–3723.

80. Khomenko, T.I., Golovina, O.A., Sakharov, M.M., Krylov, O.V., Partridge, R.D., and Weiss, A.H. (1976). Homogeneously catalyzed formaldehyde condensation to carbohydrates: IV. Alkaline earth hydroxide catalysts used with glycolaldehyde co-catalyst. J. Catal. *45*, 356–366.

81. Setsuko, I. (1984). Selective formose reaction initiated by photo- and γ-irradiation. Chem. Lett. *13*, 2153–2156.

82. Tambawala, H., and Weiss, A.H. (1972). Homogeneously catalyzed formaldehyde condensation to carbohydrates: II. Instabilities and Cannizzaro effects. J. Cat. *26*, 388–400.

83. Ball, G.F.M. (1990). The application of HPLC to the determination of low molecular weight sugars and polyhydric alcohols in foods: a review. Food Chem. *35*, 117–152.

84. Omran, A., Menor-Salvan, C., Springsteen, G., and Pasek, M. (2020). The messy alkaline formose reaction and its link to metabolism. Life (Basel) *10*, 125.

85. Shigemasa, Y., Fujitani, T., Sakazawa, C., and Matsuura, T. (1977). Formose reactions. III. Evaluation of various factors affecting the formose reaction. Bull. Chem. Soc. Jpn. *50*, 1527–1531.

86. Soares, A.P.V., Portela, M.F., and Kiennemann, A. (2007). Methanol selective oxidation to formaldehyde over iron-molybdate catalysts. Catal. Rev. *47*, 125–174. https://doi.org/10.1081/CR-200049088.

87. Millar, G.J., and Collins, M. (2017). Industrial production of formaldehyde using polycrystalline silver catalyst. Ind. Eng. Chem. Res. *56*, 9247–9265.

88. Shen, X., and Perreault, H. (1998). Characterization of carbohydrates using a combination of derivatization, high-performance liquid chromatography and mass spectrometry. J. Chromatogr. A *811*, 47–59.

89. Szeja, W., Fokt, I., and Grynkiewicz, G. (1989). Benzylation of sugar polyols by means of the PTC method. Recl. Trav. Chim. Pays-Bas *108*, 224–226.

90. Lendenmann, U., and Egli, T. (1995). Is *Escherichia coli* growing in glucose-limited chemostat culture able to utilize other sugars without lag? Microbiology (Reading) *141*, 71–78.